

# 3-Chloroanisole for overcharge protection of a Li-ion cell

Young-Gi Lee<sup>a</sup>, Jaephil Cho<sup>b,\*</sup>

<sup>a</sup> Ionics Devices Team, Electronics and Telecommunications Research Institute (ETRI), Daejeon 305-700, Republic of Korea

<sup>b</sup> Department of Applied Chemistry, Kumoh National Institute of Technology, Gumi 730-701, Republic of Korea

Received 8 March 2007; received in revised form 11 May 2007; accepted 13 June 2007

Available online 19 June 2007

## Abstract

We observed that 3-chloroanisole (3CA), as an electrolyte additive was very effective for overcharging protection during a 12 V overcharging reaction. During overcharging, the cell voltage did not increase beyond 5.3 V, as opposed to other aromatic compounds that showed a voltage shoot-up to 12 V. This behavior was due to the 3CA decomposition and the formation of conducting polymer film within separator and at cathode/electrolyte interface, which consumes the surplus current and inhibit the voltage increase through the shunting effect. In addition, the use of 3CA did not lead to any problems with rate capability, cycle life, and long-term storage behavior at 50 and 70 °C. Furthermore, during storage at 90 °C for 4 and 24 h, electrolyte with 3CA in a Li-ion cell showed a similar increase of cell thickness as a cell without 3CA.

© 2007 Elsevier Ltd. All rights reserved.

**Keywords:** 3-Chloroanisole; Electrolyte additive; Overcharge protection; Li-ion cell

## 1. Introduction

The safety concern of Li-ion batteries is important for their commercial application [1–10]. In many abuse conditions, such as overcharge and short-circuit, the electrolytes react exothermally with electrodes, resulting in thermal runaway of the Li-ion cells. Most Li-ion batteries have adopted external safety system such as integrated circuit (IC) that interrupts surplus current, a pressure-activated aluminum burst disk and current breaker, and a positive temperature coefficient (PTC) device. However, they add a cost problem to Li-ion cells and also work to permanently inactivate and even damage the battery.

As the mobile electronics requires larger Li-ion capacity, the safety problem is the most critical issue of the present Li-ion batteries. Thus, an internal safety system that operates before the cell reaches the dangerous point without inactivating the battery is also desirable. There have been several reports on a built-in and chemical prevention of the overcharge, namely, electrolyte additives [11–27].

Among them, redox shuttle compounds such as *n*-butylferrocene [15], anisole and phenothiazine [16,17] as an additive consume extra current by repetitive redox reaction between cathode and anode. When the full charge voltage is exceeded,

the redox additive in the electrolyte is oxidized at the cathode, migrates to the anode, and is reduced reversibly to the original state. These reactions occur over and over to keep the voltage steady even when an overcharge current is supplied. However, they show some limit over huge current management, so they are still not sufficient to effectively prevent overcharge.

Other additives for overcharge protection are the aromatic compounds [19–22] such as biphenyl (BP) and cyclohexyl benzene (CHB), which polymerize electrochemically at the cathode/electrolyte interface. The formed polymer film seems to act as a passive layer increasing internal impedance and eventually shutting down LIBs though some controversy on their working mechanism.

In this study, we chose 3-chloroanisole (3CA) among others because it has redox potential above 4.4 V and could readily undergo further decomposition beyond 4.6 V due to its poor delocalization of lone-pair electrons in one methoxy oxygen [28,29]. We investigated 12 V overcharge test for Li-ion cell containing 3CA as a protecting electrolyte additive. In addition, its influences for rate capability, cycle life, and long-term stability under high-temperature storage are also investigated.

## 2. Experimental

Liquid electrolytes (1M LiPF<sub>6</sub> in ethylene carbonate (EC)/dimethyl carbonate (DMC)/diethyl carbonate (DEC)

\* Corresponding author. Fax: +82 54 478 7710.  
E-mail address: [jpcho@kumoh.ac.kr](mailto:jpcho@kumoh.ac.kr) (J. Cho).

(1/1/1, w/w) (Cheil Ind., Korea) containing less than 20 ppm HF were used for electrochemical tests. 3-chloroanisole (98% purity, Aldrich) was further purified by vacuum distillation before use. The cathodes for the battery test cells (463448-size pouch type) were made from the  $\text{LiCoO}_2$  cathode material, Super P carbon black, and polyvinylidene fluoride (PVdF) binder (Kureha Company) in a weight ratio of 96:2:2. The anodes for the battery test cells were made from the synthetic graphite powders, and polyvinylidene fluoride (PVdF) binder (Kureha Company) in a weight ratio of 94:6. The electrodes were prepared by coating a cathode-slurry onto an Al foil followed by drying at  $130^\circ\text{C}$  for 20 min. The slurry was prepared by thoroughly mixing an *N*-methyl-2-pyrrolidone (NMP) solution of PVdF, carbon black, and the powdery cathode material. The test cells were aged at room temperature for 24 h prior to the electrochemical test. Li-ion cells with a nominal capacity of 700 mAh were used for the electrochemical tests and 12 V overcharging experiments. The dimensional ratio of anode to cathode of 1.08:1 was used for the Li-ion cells. The overcharge test was conducted with a constant current of 1 A. The cell-surface temperature was monitored using a K-type thermocouple placed on the center of the largest face in the cell can, and the thermocouple was tightly glued with insulating tape. For the rate capability and life cycle performance tests, the cells were charged with a constant current mode to 4.2 V and maintained at this voltage with a constant voltage mode (CV) for 5 h. For the storage tests, the cells were charged with CC mode to 4.2 V and maintained at this voltage with a constant voltage mode (CV) for 5 h. After fully charging to 4.2 V, the cells were kept at 4.2 V at various temperatures.

Cyclic voltammogram experiments were carried out with a Solartron 1287 potentiostat/galvanostat using a three-electrode cell. A 2 mm diameter Pt disk was used as the working electrode, a Pt plate as counter electrode, and lithium pressed on a SUS strip was used as a reference electrode. The potentials are shown in reference to the lithium versus  $\text{Li}/\text{Li}^+$ . The scan rate for linear sweep voltammetry (LSV) experiment was 2 mV/s. The  $^1\text{H}$  NMR spectra were obtained in dimethylsulfoxide ( $\text{DMSO}-d_6$ ) or chloroform-*d* ( $\text{CDCl}_3$ ) solvent on a Bruker-AMX 500 NMR spectrometer with tetramethylsilane (TMS) as an internal standard.

### 3. Results and discussion

Fig. 1 shows profiles of cell voltage and cell surface temperature during the overcharging test using Li-ion cells containing electrolytes without 3CA and with 3 and 5 wt.% 3CA. One main feature of Fig. 1(a) during the overcharge test is the steep voltage uprise above 6 V (up to 12 V). The internal temperature can increase above the melting temperature of polymer separator ( $T_m = 120\text{--}150^\circ\text{C}$ ), accompanied by a separator shutdown and a rapid increase in the cell resistance. Moreover, further increase of internal temperature even can melt down separator and the Li metal ( $T_m = 180^\circ\text{C}$ ) deposited on the anode. Then, the cell leads to internal short circuit in the end as shown in Fig. 1(a). After 25 min cell voltage abruptly decreases to almost 0 V. Therefore, an internal short circuit resulted from overcharging directly leading to the thermal runaway of the Li-ion cell,

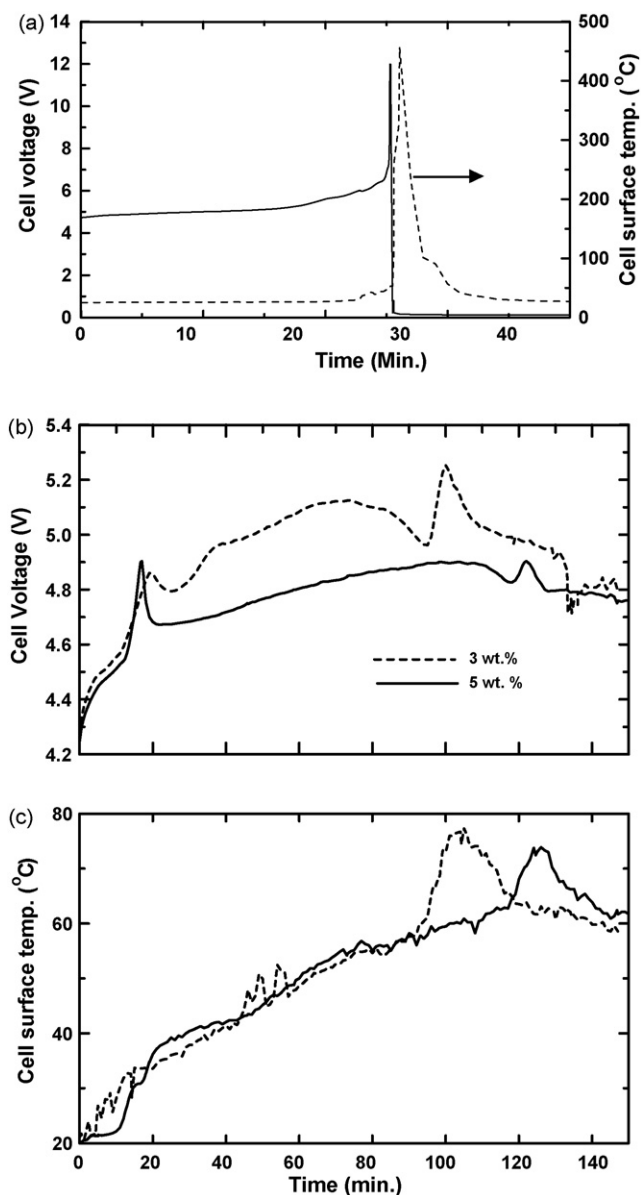


Fig. 1. Profiles of cell voltage during 12 V overcharging test for using Li-ion cells containing electrolytes: (a) without 3CA, (b) with 3 and 5 wt.% 3CA, and (c) cell-surface temperatures of (a) and (b).

accompanied with a fire and an explosion. In addition, melting of the deposited lithium metal significantly accelerated the thermal runaway of the cell. After shoot-up to 12 V, the voltage profile of the cell without 3CA shows a sharp drop to 0 V with a maximum cell-surface temperature of approximately  $450^\circ\text{C}$ . This study found that the five tested cells were destroyed and covered with soot as a result of fire and explosion. This is due to an instant internal short-circuit of the cell after the 12 V maximum. On the other hand, cells containing 3 wt.% 3CA did not show an increase of cell voltage over 5.3 V and the cell surface temperatures did not increase over  $80^\circ\text{C}$ . As can be seen in Fig. 1(b), after a less abrupt voltage increase up to 4.9 V compared to Fig. 1(a), the voltage was sustained below 5.3 V for the entire 150 min. Coinciding with this, the cell-surface temperature reached its maximum of  $80^\circ\text{C}$  around 100 and 120 min

in which the voltage reached the maximum point in Fig. 1(c). The cell containing 5 wt.% 3CA showed a maximum cell voltage of 4.9 V with a similar cell-surface temperature as the cell containing 3 wt.% 3CA. As a result, 3CA demonstrated excellent overcharge protection behavior. However, 3CA is a redox shuttle-type additive around 4.5 V thus it would not be able to effectively protect overcharge behavior over 5 V and even 12 V. In addition, Fig. 1(b and c) shows typical film-forming additive's voltage profile. So, we expect that 3CA also could be oxidized to form a poly(*p*-phenylene)-type derivatives through the radical coupling mechanism [25–27]. Since the polymerized protective film has its electronic conductivity, it could show shunting effect (soft short circuit). Accordingly, this shunting effect lead to consume surplus currents and to inhibit the voltage increase through formed conductive polymers between anode and cathode, on the separator surface, within the pores, and at cathode/electrolyte interface, etc. Dahn group already suggested that anisoles can be good redox shuttle agents [17]. His group mainly focused on redox shuttle reaction within voltage cut-off range, 3.0–4.5 V without showing any further study above 5 V. However, we notice that anisole-type redox shuttle agent also can act as film-forming additive like BP and CHB. Unlike other conventional anisoles, 3CA is not effective as a redox shuttle agent within cut-off range or below 4.6 V. As a result, 3CA did not show any redox shuttle effect though similar structure with other anisoles. Instead, we think that film forming effect by decomposition and polymerization of 3CA is responsible for the improved overcharge behavior.

In order to understand this result,  $^1\text{H}$  NMR and the linear sweep voltammetry (LSV) analyses were performed for the 3CA containing samples. Fig. 2(a) shows the  $^1\text{H}$  NMR spectrum of the electrolyte containing 3 wt.% 3CA as a reference before overcharging.  $^1\text{H}$  NMR spectra of the liquid electrolytes extracted from the cells with 3 and 5 wt.% 3CA contents in the electrolytes after the overcharging experiment were investigated as illustrated in Fig. 1(b and c), respectively. In Fig. 2(a), the peaks at 6.85–7.35 ppm were assigned to all four aromatic res-

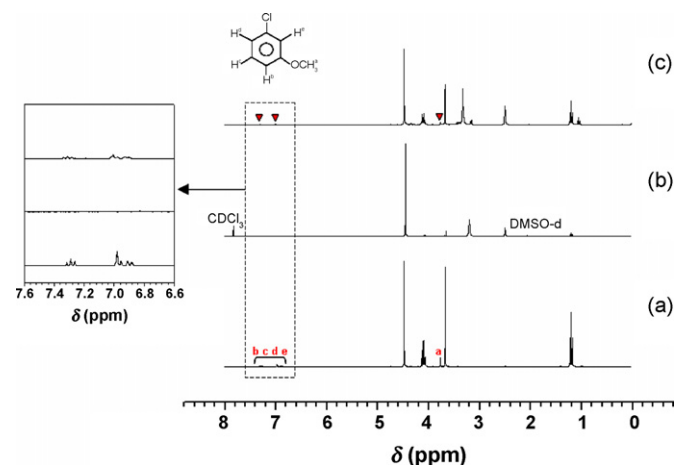


Fig. 2. Plots of (a)  $^1\text{H}$  NMR spectrum of pure 1 M  $\text{LiPF}_6$  in EC/DMC/DEC containing 3 wt.% 3CA as a reference before overcharging, and (b) and (c)  $^1\text{H}$  NMR spectra of the liquid electrolytes extracted from the cells containing 3 and 5 wt.% 3CA, respectively, in the electrolytes after the overcharging experiment.

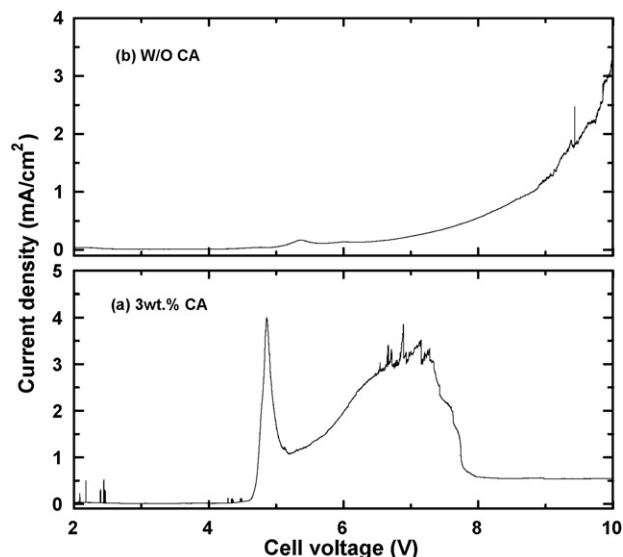


Fig. 3. Linear sweep voltammogram (LSV) was performed for 1 M  $\text{LiPF}_6$  in EC/DMC/DEC. (a) Containing 3 wt.% 3CA and (b) without 3CA as a reference.

onate protons (peaks b–e) in benzene and the peak appearing at 3.77 ppm corresponded to the methoxy proton (peak a), that is, a substitute on the three-position of benzene in 3CA. For conventional redox additives, the additive concentration should be maintained without any decomposition when locking the cathode potential during overcharging. However, as seen in Fig. 2(b and c), 3CA peaks disappeared in Fig. 2(b) and show only traces ( $\blacktriangledown$ ) in Fig. 2(c) demonstrating that 3CA decomposed after overcharging. We assume that this decomposition reaction could be strongly related with the polymerization reaction of 3CA at the separator surface, within the pores, and the cathode/electrolyte interface [18–22].

To illustrate that the disappeared 3CA peaks in the NMR data are correlated to the decomposition of 3CA, linear sweep voltammograms (LSV) were measured for the electrolyte containing 3 wt.% 3CA and the electrolyte without 3CA as a reference in Fig. 3(a and b), respectively. Fig. 3(a) shows two oxidation peaks with the first sharp peak around 4.5 V and the second broad peak ranging from 5.5 to 8 V. Afterwards, it shows constant current behavior. However, the oxidation current for the normal electrolyte without 3CA remains steady up until 5.5 V and then gradually and continuously increases, which indicates that the electrolytes without 3CA were decomposed. Thus, it can be concluded that the first narrow peak in Fig. 3(a) is due to oxidation of 3CA as redox shuttle reaction, not decomposition of 3CA and the second broad peak may originate from the decomposition of 3CA to reach for electrochemical polymerization and partially electrolyte decomposition induced by the decomposed 3CA. It is known that most anisoles as redox shuttle agents have two methoxy substitutes and one halogen substitute on the benzene ring. They show typical redox shuttle behavior and very stable because the lone-pair electrons of the two methoxy oxygens in the canonical structure can take part in the delocalization of electrons. Thus, the spatial delocalization makes the oxidized compounds fairly stable [28,29]. On the other hand, lone-pair electrons of one methoxy oxygen in 3CA cannot take part in the

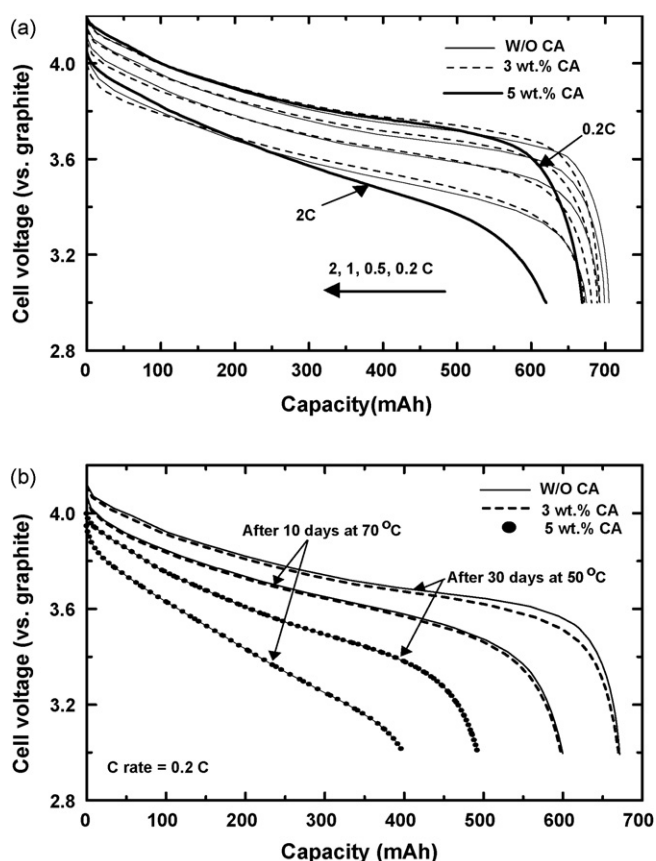


Fig. 4. Voltage profiles of the (a) rate capability and (b) capacities of the cell containing 3 and 5 wt.% CA and without CA after storage at 60 and 70 °C for 30 and 10 days, respectively. For the rate capability tests, the charge rate was fixed at 0.5 C and the discharge rate increased from 0.2, 0.5, 1 and 2 C.

delocalization effectively. Thus, oxidized 3CA would readily undergo further decomposition beyond 4.6 V.

Fig. 4(a and b) show the voltage profiles of the rate capability and capacities of the cells containing 3 wt.% 3CA and without 3CA after storage at 60 and 70 °C for 30 and 10 days, respectively. After storage, the cells were charged to 4.2 V using same charging method to as described in experimental Section 2 and discharged to 3 V at a rate of 0.2 C at room temperature to see the capacity recovery. The rate capability of the cell with 3CA showed that capacity retention at the 2 C rate was quite similar (97%) to that without 3CA compared to the capacity at 0.2 C. Similar to this, the capacity recovery of the cell containing 3CA was also quite similar to that without 3CA, indicating that 3CA addition into the electrolyte affected neither rate capability nor storage recovery. However, we observed that 5 wt.% CA addition decreased the rate capability and capacity

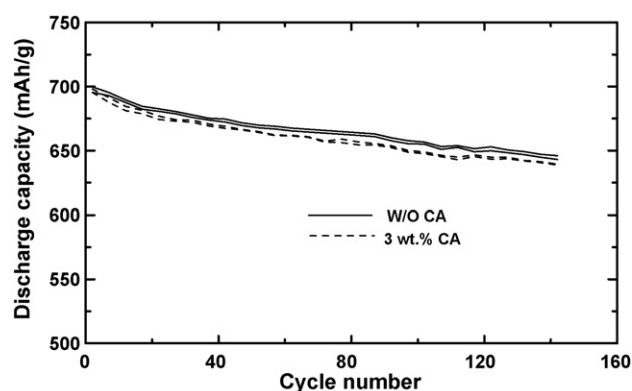


Fig. 5. Plot of capacity retention of the cell containing 3 wt.% 3CA and without 3CA out to 160 cycles at a 1 C rate at 25 °C. The cell charge and discharge cut-off voltages were 4.2 and 3 V, respectively.

recovery at 70 °C by 30%, compared with 3 wt.% CA. Cycle life testing of the cells containing 3 wt.% 3CA at a 1 C rate also demonstrated excellent performance up to 160 cycles at 25 °C, showing a similar capacity retention value of 93%, compared with the cell without 3CA, as shown in Fig. 5. Since the potential disadvantage of 3CA might be the self-discharge of the cell at high voltage, we measured the leakage currents of the Li-ion cells containing the 3CA (3 and 5 wt.%) and without 3CA at room temperature at 4.2 V. After equilibrating the cell at 4.2 V using the Li-ion cells, the leakage currents were measured after 1 h according to the method reported by Conway et al. [30] the measured current of the cell with and without 3CA (3 wt.%) was 0.01 mA. However, when 3CA content in the electrolyte was increased to 5 wt.%, its value was to 0.04 mA. The result indicates that 3 wt.% CA addition to the electrolyte is not problematic.

The most critical parameter for feasibility in practical applications of the additive is to evaluate its use at 90 °C for 4 h in the charged state because the additives at this temperature after charging may vigorously decompose. As shown in Table 1 (tests were conducted after charging to 4.2 V), we compared cell impedance, open cell voltage (OCV), and thickness change after storage at 90 °C for 4 and 24 h using Li-ion cells containing 3 wt.% 3CA and normal electrolyte (without 3CA) cells. Three weight percent 3CA addition to the electrolyte shows negligible effects on the cell impedance and OCV. Although, it is rather difficult to measure the cell thickness by using soft Al-laminated pouches, we observe increase in cell thickness upon storage at 90 °C (cell thickness was measured from the center part of the cell). However, after 24 h storage, although all the measured parameters increase sharply, the values of the cell with and without 3CA are quite similar to each other.

Table 1

Cell impedance, open cell voltage, and thickness change after storage at 90 °C for 4 h using Li-ion cells containing 3 wt.% CA and normal electrolyte (without 3CA)

Sample name	Initial			After 4 h (24 h) at 90 °C		
	Cell impedance (ohm)	OCV (V)	Thickness (mm)	Cell impedance (ohm)	OCV	Thickness
Without 3CA	53	4.19	4.7 (5.4)	59 (89)	4.11 (4.02)	5.1 (5.6)
With 3CA	54	4.19	4.7 (5.5)	60 (87)	4.10 (4.03)	5.1 (5.6)

#### 4. Conclusions

3CA additive demonstrated excellent overcharge protection behavior, blocking voltage increases above 5.3 V as opposed to other aromatic compounds. This was due to the continuous current consumption from 3CA decomposition and consecutively formed conducting polymer film within separator and at cathode/electrolyte interface. Although, redox shuttle reactions occurred earlier within the cut-off voltage range, they had no influence on the normal cycle behavior between 3 and 4.2 V and the cell showed excellent cycle life performance and storage characteristics at 60, 70, and 90 °C.

#### Acknowledgement

This study was supported by Research Fund, Kumoh National Institute of Technology.

#### References

- [1] H. Maleki, A. Said, J.R. Selman, R. Dinwiddie, H. Wang, *J. Electrochem. Soc.* 146 (1999) 947.
- [2] K. Kanari, *Prog. Batteries Battery Mater.* 16 (1997) 316.
- [3] A. Du Pasquier, F. Disma, T. Bowmer, A.S. Gozdz, G. Amatucci, J.-M. Tarascon, *J. Electrochem. Soc.* 145 (1998) 472.
- [4] H. Maleki, G. Deng, A. Anani, J. Howard, *J. Electrochem. Soc.* 146 (1999) 3224.
- [5] S.C. Levy, P. Bro, *Battery Hazards and Accident Prevention*, Plenum Press, New York, 1994.
- [6] K. Kitoh, H. Nemoto, *J. Power Sources* 81 (1999) 887.
- [7] R.A. Leising, M.J. Palazzo, E.S. Takeuchi, K.J. Takeuchi, *J. Electrochem. Soc.* 148 (2001) A838.
- [8] K. Xu, M.S. Ding, S. Zhang, J.L. Allen, T.R. Jow, *J. Electrochem. Soc.* 149 (2002) A622.
- [9] J. Cho, Y.W. Kim, B. Kim, B. Park, *Angewandte Chemie (international edition)* 42 (2003) 1618.
- [10] J. Cho, J.-G. Lee, B. Kim, B. Park, *Chem. Mater.* 15 (2003) 3190.
- [11] C.W. Lee, R. Venkatachalapathy, J. Prakash, *Electrochem. Solid-State Lett.* 3 (2000) 63.
- [12] S. C. Narang, S. C. Ventura, B. J. Dougherty, M. Zhao, S. Smedley, G. Koolpe, U.S. Patent 5,830,600 (1998).
- [13] X. Wang, E. Yasukawa, S. Kasuya, *J. Electrochem. Soc.* 148 (2001) A1058.
- [14] N. Takami, T. Ohsahi, H. Hasebe, M. Yamamoto, *J. Electrochem. Soc.* 149 (2002) A9.
- [15] K.M. Abraham, *Electrochim. Acta* 38 (1993) 1233.
- [16] C. Buhrmester, J. Chen, L. Moshurchak, J. Jiang, R.L. Wang, J.R. Dahn, *J. Electrochem. Soc.* 152 (2005) A2390.
- [17] C. Buhrmester, L. Moshurchak, R.L. Wang, J.R. Dahn, *J. Electrochem. Soc.* 153 (2006) A288.
- [18] X. Feng, X. Ai, Y. Cao, H. Yang, *J. Appl. Electrochem.* 34 (2004) 1199.
- [19] L. Xiao, X. Ai, Y. Cao, H. Yang, *Electrochim. Acta* 49 (2004) 4189.
- [20] S. Tobishima, Y. Ogino, Y. Watanabe, *J. Appl. Electrochem.* 33 (2003) 143.
- [21] Y. Watanabe, H. Morimoto, S. Tobishima, *J. Power Sources* 154 (2006) 246.
- [22] H. Lee, J.H. Lee, S. Ahn, H.-J. Kim, J.-J. Cho, *Electrochem. Solid-State Lett.* 9 (2006) A307.
- [23] U.S. Patent #5,709,968 (1998).
- [24] Japan Patent #3,669,024 (2005).
- [25] M. Satoh, K. Imanishi, K. Yoshino, *J. Electroanal. Chem. Interfacial Electrochem.* 317 (1991) 139.
- [26] L.M. Goldenberg, P.C. Iacaze, *Synth. Met.* 58 (1993) 271.
- [27] H. Lee, S.-Y. Cui, S.M. Park, *J. Electrochem. Soc.* 148 (2001) D139.
- [28] M. Adachi, K. Tanaka, K. Seika, *J. Electrochem. Soc.* 146 (1999) 1256.
- [29] U.S. Patent #6,045,952 (2000).
- [30] B.E. Conway, W.G. Pell, T.-C. Liu, *J. Power Sources* 65 (1997) 53.